

Structural and Optical Properties of Polymer Blend Nanocomposites Based on Poly (vinyl acetate-co-vinyl alcohol)/TiO₂ Nanoparticles

A. Ismaila¹, P. O. Akusu¹ and T. O. Ahmed^{2*}

¹Department of Physics, Ahmadu Bello University, Zaria, Nigeria

²Department of Physics, Federal University Lokoja, Kogi, Nigeria

Research Article

13

ABSTRACT

Titanium dioxide and organic polymer blend poly (vinyl acetate-co-vinyl alcohol) based nanocomposite membranes were prepared and their chemical structure, phase relationship and optical properties investigated. The Scanning Electron Microscopy (SEM) coupled with Energy Dispersive X-ray Spectroscopy (EDS) analysis reveals TiO₂ to be almost isomorphic ($\geq 99\%$ phase purity) with spherical particles having diameters in the range 25-40nm. The composites were characterized by Fourier Transform Infra Red (FTIR), SEM, X-Ray Diffraction (XRD) and Ultraviolet-visible (UV-vis) Spectrophotometry. The FTIR Spectroscopy reveals significant absorptions below 900cm⁻¹ to represent Titanium bonds with organic groups and Oxygen while other prominent functional groups above 900cm⁻¹ reflect the additivity of polyvinyl alcohol and polyvinyl acetate. It was found that embedding inorganic nanoparticles of TiO₂ into the polymer blend matrix of poly (vinyl acetate-co-vinyl alcohol) allowed for some crystallinity formation and cross-linking of the polymer composites during annealing. The XRD results show more defined peaks assigned to each phase of the composite as the TiO₂ content increases from 1 to 4% weight ratio, thus indicating that Nanoparticle filler remain in the semi-crystalline polymer matrix as a separate crystalline phase, which is in good agreement with the SEM. Finally, the resonant coupling between le (UV-vis) light and the collective electronic transitions of polymer nanocomposites are examined using UV-vis Spectrophotometer. The variation in the percentage absorbance and transmittance over wavelength range 200nm-900nm is also attributed to TiO₂ Nanoparticles (Nps) content (1-4%) in the samples.

Keywords: Polymer blend; TiO₂ Nanoparticles; Polymer Nanocomposites; Chemical structure; UV-visible light absorber.

* Tel.:

E-mail address: tajahmol@yahoo.co.uk; tajahmol@gmail.com.

29 **1. INTRODUCTION**

30

31

32

33

34

35

36

37

38

39

40

41

42

43

44

45

46

47

48

49

50

51

52

53

54

55

56

57

58

59

60

61

62

63

64

65

66

67

68

69

70

71

72

73

74

75

76

77

78

79

80

In the last few years, the prospects for polymer blending have been compared to the alloying of metals because it requires little or no extra capital expenditure compared to the production of new polymers. This leverage has led to extensive use of polymer blends in the polymer industry over the last few years. Also, polymer blending offers the possibility of producing a range of polymeric materials with properties completely different from those of the blend constituents [1]. Blend properties are crucially affected by phase morphology and this in turn depends upon a number of factors including the choice of parent polymers, compatibilizers, blend composition, moisture content and the method of blend preparation [2,3]. Because of the significant interest in interfacial interaction between inorganic and organic phases (such as variety of polymer and their blend derivatives) as well as size-dependent phenomena of nanoscale particles, polymer blend nanocomposites are capable of dramatically improving numerous favorable properties without losing the inherent good properties of the polymer phases such as ductility, optical transparency etc. these advantages are never achieved in the conventional polymer composites. In addition, property enhancements in polymer nanocomposites are achieved at a very low loading (<5 wt %) of inorganic nanoparticles while the conventional polymer composites (polymer containing microparticles/micron-sized particles as fillers) usually require much loading of the order of 25-40 wt % [4].

In contrast to the traditional dyes, inorganic semiconductive nanocrystals have more resistant to chemical attacks and low degradation with higher photobleaching, broader excitation wavelength range, narrower and tunable emission spectra [5,6,7,8]. This influence has attracted an enormous research effort leading to a myriad of potential applications in engineering, medicine, biology, electronics and allied industries. Their optical properties have been the center of attraction due to strong size-dependent quantum confinement effect associated with inorganic semiconductive nanocrystals. For the development of novel nanodevices such as electronics and optical devices, various stabilizers (surfactants, polymers or coupling agents) have been employed to modify the surface functionalities of the nanocrystals [9,10], as these nanocrystals are seldom prepared without aggregation. A great deal of attention has been focused on TiO₂ in contrast to other semiconducting materials, because of its low cost, non-toxicity, chemical stability, resistance to photocorrosion, high photocatalytic activity and high refractive index [11,12]. In the last decade, most studies are mainly focused on the dispersion of nanocrystalline TiO₂ powder for photocatalysis compared to TiO₂ thin films due to its higher photocatalytic activity [13]. It is an established fact that a mixture of anatase TiO₂ and a small percentage of rutile TiO₂ give optimal photocatalytic efficiency as the anatase phase has a wider band gap of 3.20 eV [14].

Polymer nanocomposites represent a merger between traditional organic and nanosized inorganic materials, resulting in compositions that are truly hybrid. The key to forming such novel materials is adequate understanding and manipulation of the guest-host chemistry, occurring between the polymer and the nanoparticles, in order to obtain a homogenous dispersion and a good contact between polymer and added particle surfaces [15]. Generally, the resultant nanocomposites display enhanced favorable properties such as conductivity, toughness, optical activity, catalytic activity, chemical selectivity etc [16]. These attributes have led to the growing interest and uses in various fields such as military equipments, safety and protective garments, automotive, aerospace, electronic and optical devices. A lot of research works exploiting these aforementioned properties have been carried out for possible applications including flame retardancy, chemical resistance, UV resistance, electrical conductivity, environmental stability, water repellency, magnetic field resistance, radar absorption etc [17, 18, 19, 20, 21].

81

82 In this paper, we report the development of Poly (vinyl acetate-co-vinyl alcohol)/TiO₂
83 nanocomposites achieved via a two-stage synthetic route and the relationship between
84 structural and optical properties of the resulting hybrid Poly(vinyl acetate-co-vinyl
85 alcohol)/TiO₂ nanocomposites employing Fourier Transform Infrared (FTIR) spectroscopy,
86 Scanning Electron Microscopy (SEM), X-Ray Diffraction (XRD) analysis and UV-visible
87 Spectrophotometry.

88

89

90

91 2. MATERIAL AND METHODS

92

93 Poly (vinyl acetate-co-vinyl alcohol)/TiO₂ nanocomposites were produced via a two-stage
94 reaction involving the synthesis of TiO₂ Nanoparticles (Nps) from titanium (IV) chloride
95 {TiCl₄, BDH Limited Poole, England} employing hydrothermal technique and subsequent
96 mixing of modified TiO₂ Nps with Poly(vinyl acetate-co-vinyl alcohol) dissolved in toluene via
97 one-pot reaction. Surface morphology of the synthesized TiO₂ nanoparticles was observed
98 using EVOI MA10 (ZEISS) multipurpose scanning electron microscope operating at 20kV
99 employing secondary electron signals. Four samples of Poly (vinyl acetate-co-vinyl
100 alcohol)/TiO₂ nanocomposites containing 1-4% of TiO₂ Nps were produced by solution
101 casting into Petri dishes. The samples were oven dried at temperature lower than the
102 melting point of the polymer blend for 12hrs and subsequently flat and uniform thin samples
103 were obtained. The FTIR spectra of all the component reagents, polymer blend and the
104 prepared nanocomposite samples were obtained using SHIMADZU FTIR-8400S
105 Spectrophotometre in transmission mode without KBr. The spectra were recorded in the
106 frequency range from 400 to 4600 cm⁻¹, after 25 scans, with resolution of 2cm⁻¹. The
107 positions and intensities of the IR bands were processed with Spectral Analysis software.

108 Surface morphologies of Poly (vinyl acetate-co-vinyl alcohol)/TiO₂ nanocomposites were
109 observed using EVOI MA10 (ZEISS) multipurpose scanning electron microscope operating
110 at 20kV employing secondary electron signals at a magnification of 500X and the particle
111 size distribution was obtained using imaging software (Image-J). The crystallinity of polymer
112 blend/TiO₂ nanocomposites was observed using X-Ray Diffractometre (Phillips X'pert Pro X-
113 Ray Diffractometre) employing a 1.54060Å copper X-ray source. The samples were scanned
114 from 2θ = 5°-80° using a step size of 0.06°. The percentage crystallinity (X_c) was calculated
115 following the procedure proposed by [22], with the Scientific Graphing and Data Analysis

116 Software (Origin 8.0), using the following equation: $X_c = \frac{A_c}{A_c + A_a}$ where X_c, (percentage

117 crystallinity), is the ratio of crystalline peak area (A_c) to the sum of the crystalline peak area
118 (A_c) and amorphous peak area (A_a). Finally, the absorption/filtering property of the polymer
119 blend /TiO₂ nanocomposites was studied in the ultraviolet (UV) radiation wavelength range
120 of 200nm-400nm and visible radiation wavelength range of 400nm-900nm using JENWAY
121 6405 UV-visible Spectrophotometre.

122

123

124 3. RESULTS AND DISCUSSION

125

126 The image presented in figure 1 together with the corresponding EDS spectra obtained
127 using characteristic x-rays emitted by TiO₂ nanoparticles was observed at a magnification of
128 83.04kX. The uniform contrast in the image revealed TiO₂ to be almost isomorphic.

129 Nevertheless, Oxygen and Nitrogen occur with minor concentrations as impurities thereby
130 making Ti the dominant element with concentration of about 99.5% as depicted in the EDS
131 spectra (fig 1b). The morphology of TiO₂ nanoparticles is such that the particles are closely
132 packed and spherical in shape. The average diameter of the particles is in the range of 25-
133 40nm reflecting that TiO₂ nanoparticles are transparent and suitable filler for polymer
134 composite applications.

135

136

137

138

139

140

141

142

143

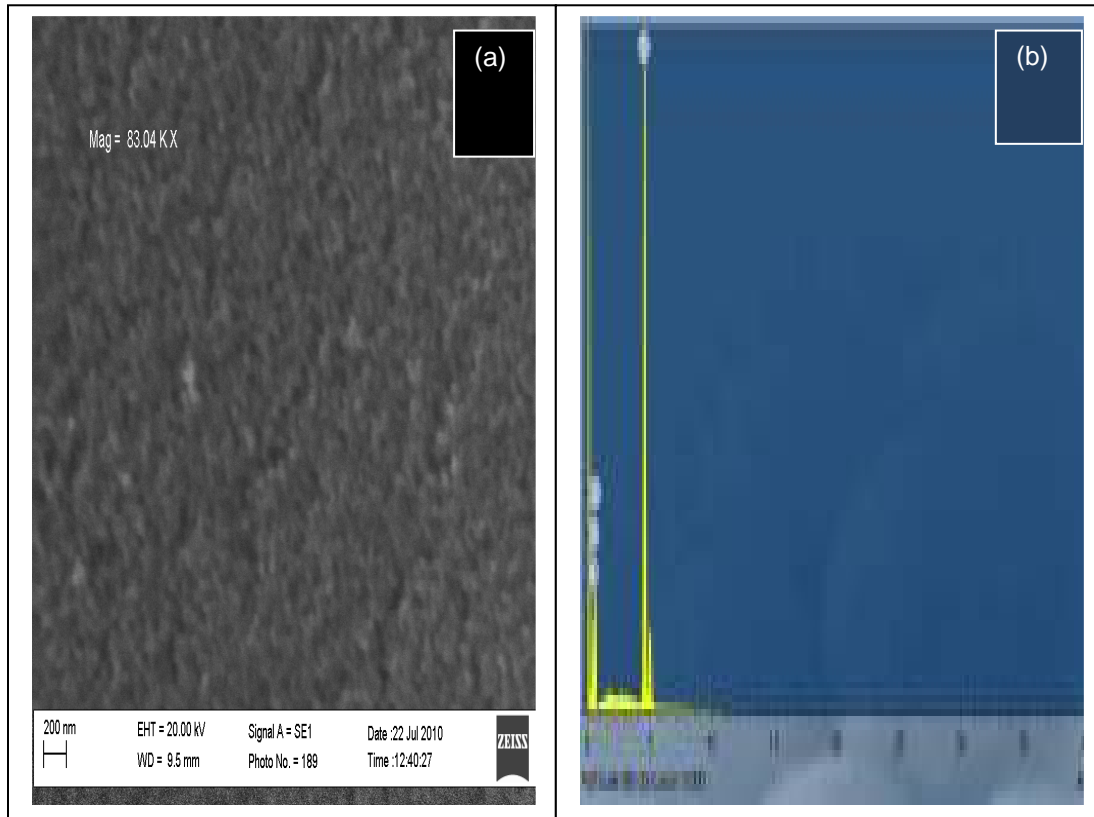
144

145

146

147

148



149

Figure 1: Microstructure and elemental composition of TiO₂ Nps: (a) SEM image of TiO₂ Nps

150

(b) EDS spectra of TiO₂ Nps.

151

152

153

154

155

156

157

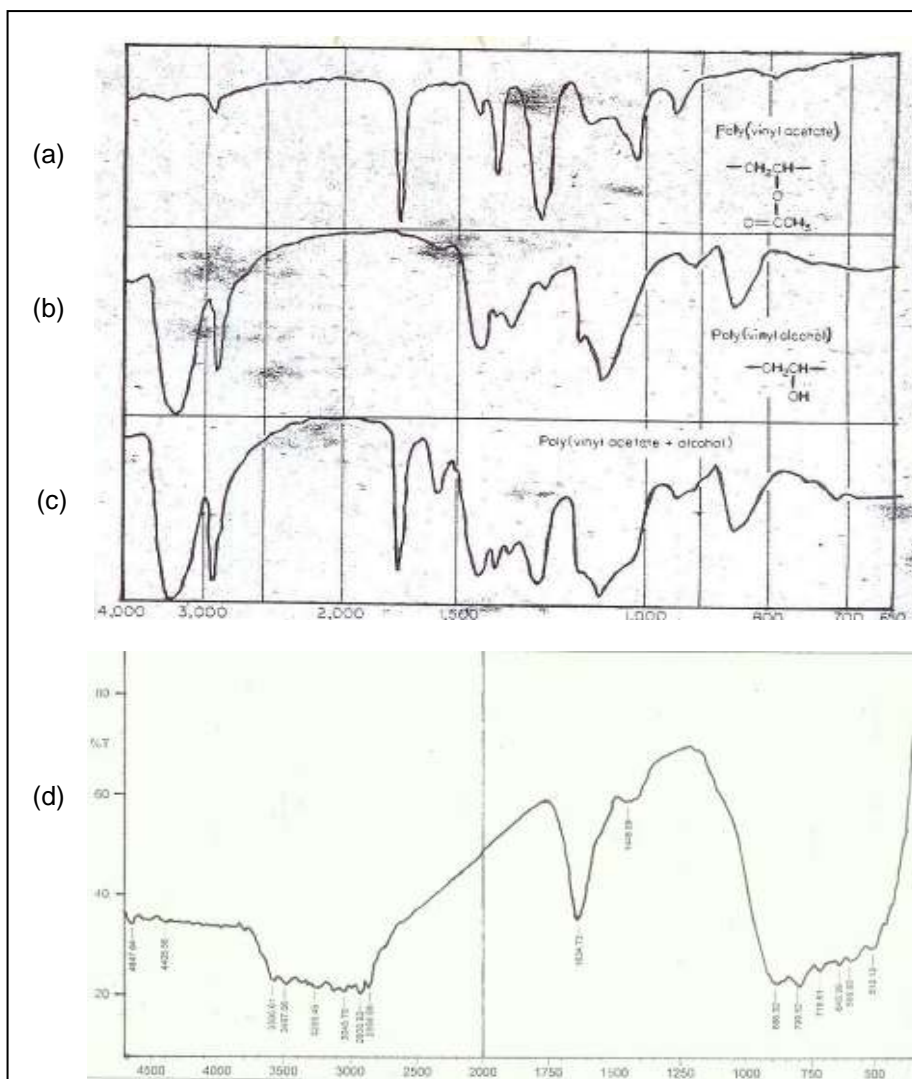
158

159

160

161

The spectra for the functionalized TiO₂ nanoparticles, poly (vinyl alcohol), poly (vinyl acetate), polymer blend [poly (vinyl acetate-co-vinyl alcohol)] and the functionalized TiO₂ are given in figure 2 (a-d) below. It is an established fact that the fundamental vibrations of solids (finger prints) are localized in the low frequency region (<1200cm⁻¹) of the midrange (400-4000cm⁻¹) of the infrared (IR) spectrum. Also, as reported by [23], the Ti-O bond is clearly located in the range from 400-900cm⁻¹. In this work, the significant absorptions observed below 900cm⁻¹ represent Ti bonds with vinyl groups, secondary alcohols, carbonyl groups and oxygen. The prominent functional groups in poly (vinyl alcohol), poly (vinyl acetate) and their blend are OH stretching vibrations, CH₂ stretching and bending vibrations, CH₃ bending vibrations, C-O-C vibration in esters, vC=O stretching vibration, C-OH stretching vibrations, CH bending and C=O stretching vibration.



162

163

164

165

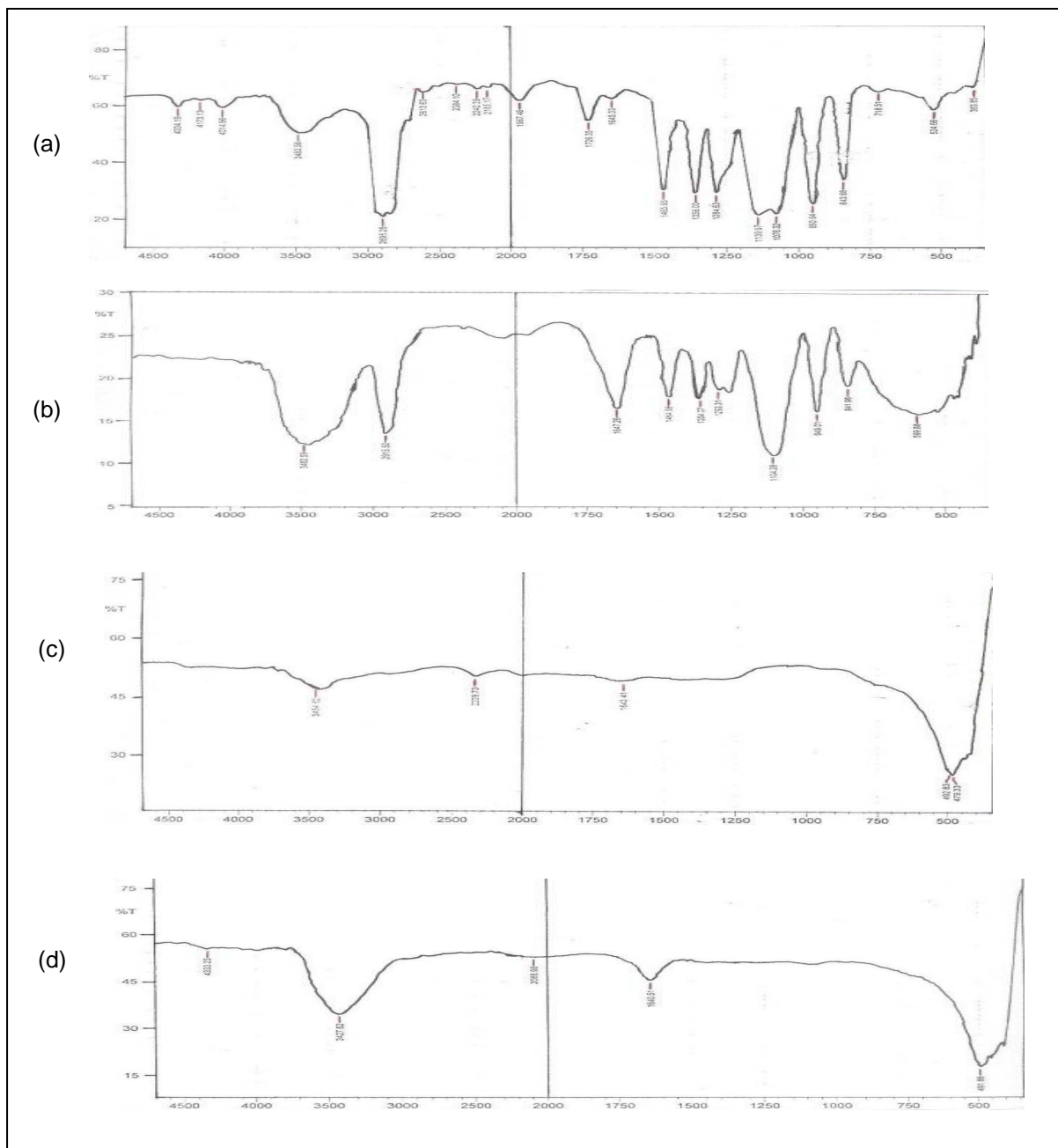
166

Figure 2: FTIR Spectra of (a) Poly(vinyl alcohol), (b) Poly(vinyl acetate), (c) Polymer blend [poly(vinyl acetate-co-vinyl alcohol)] and (d) functionalized TiO₂ Nps.

167 From figure 3(a-d), it can equally be deduced that the OH stretching vibrations of the
 168 intermolecular hydrogen bonding occurring in the range 3427.62cm⁻¹-3483.56cm⁻¹ is
 169 basically due to the adsorbed H-O-H. Organics (methylene groups) are also represented by
 170 the v_{as}-CH₂ asymmetrical stretching vibrations in ranges slightly above 2910cm⁻¹. The CH
 171 stretching vibrations with coexisting terminal triple bonds resulting from remnant alkynes
 172 occur in the range 2067.76cm⁻¹-2145.88cm⁻¹. All the changes observed in the vibration
 173 frequency of νC=O in the blend indicates that the incorporation of the nanofillers (TiO₂) has
 174 great influence on the vibration frequency of νC=O. Furthermore, conjugation with CH₃
 175 (phenyl groups) results in an increase in bond length of C=O thereby creating functional
 176 sites on the surface of the polymer blend. The C-O-C vibrations in esters occurring in the
 177 frequency ranges 949.01cm⁻¹-950.94cm⁻¹ and 1284.63cm⁻¹-1293.31cm⁻¹ represent the
 178 possible combination of acetate and alcohol groups. Finally, the functional groups appearing

179 in the range 383.85cm^{-1} - 491.66cm^{-1} represent Ti-O bonds of the functionalized TiO_2
180 nanoparticles. The observed spectra of the polymer-blend/ TiO_2 nanocomposites reveal the
181 additivity of the spectra of polyvinyl alcohol and poly vinyl acetate with the modified TiO_2
182 Nps. In figures 3(a) and 3(b), most of the functional groups peculiar to the component
183 reagents were observed but in figures 3(c) and 3(d), chemical reactions between the
184 component reagents and the increase in the concentration of the functionalized TiO_2
185 nanoparticles from 2%-4% are responsible for the extinction of the functional groups as a
186 result of oxidation and hydrolysis.

187



188

189

190

191

192

193

194

Figure 3: FTIR Spectra of Polymer blend/ TiO_2 Nanocomposites containing: (a) 1% of TiO_2 Nps (b) 2% of TiO_2 Nps (c) 3% of TiO_2 Nps and (d) 4% of TiO_2 Nps.

195 The uneven baseline in the XRD patterns seen in figure 4 (a-d) for all the samples is due to
196 the large amount of amorphous polymer content. The addition of TiO₂ nanoparticles to the
197 polymer blends improved the crystallinity of the composites. The diffraction peaks in the
198 range $2\theta = 15^{\circ}$ - 20° can be linked to crystalline behaviour of the polymer blends. The peaks
199 at $2\theta = 19.66^{\circ}$, 19.84° , 20.34° , and 20.49° with d-spacings $d = 4.5154\text{\AA}$, 4.4742\AA , 4.3642\AA
200 and 4.3325\AA indicate the presence of crystalline structure of PVA, consistent with the works
201 of [24, 25]. Furthermore, the XRD patterns of polymer blend/TiO₂ nanocomposites reveal the
202 presence of TiO₂ phase but few peaks representing TiO₂ phase have been shifted slightly to
203 lower 2θ values ($2\theta = 21.91^{\circ}$, 22.13° , 22.37° , 22.45° , 22.78° , 22.80° and 22.99°) due to slight
204 expansion of TiO₂ crystal structure as a result of surface modification and bonding with the
205 polymer blend matrix. This is also consistent with the results presented in some literatures
206 [26, 27]. The average crystallite size corresponding to structural order of the pattern
207 determined from integral breadth of the peaks according to Scherrer's equation [28] have
208 values ranging from $1688\pm 290\text{nm}$ to $4589\pm 130\text{nm}$. The percentage crystallinity values of the
209 polymer blend/TiO₂ nanocomposites following the procedure proposed by [22] range from
210 $56.9 \pm 0.2\%$ to $67.6 \pm 0.7\%$. The sample with 4% TiO₂ content displayed higher percentage
211 crystallinity compared to other samples.

212

213

214

215

216

217

218

219

220

221

222

223

224

225

226

227

228

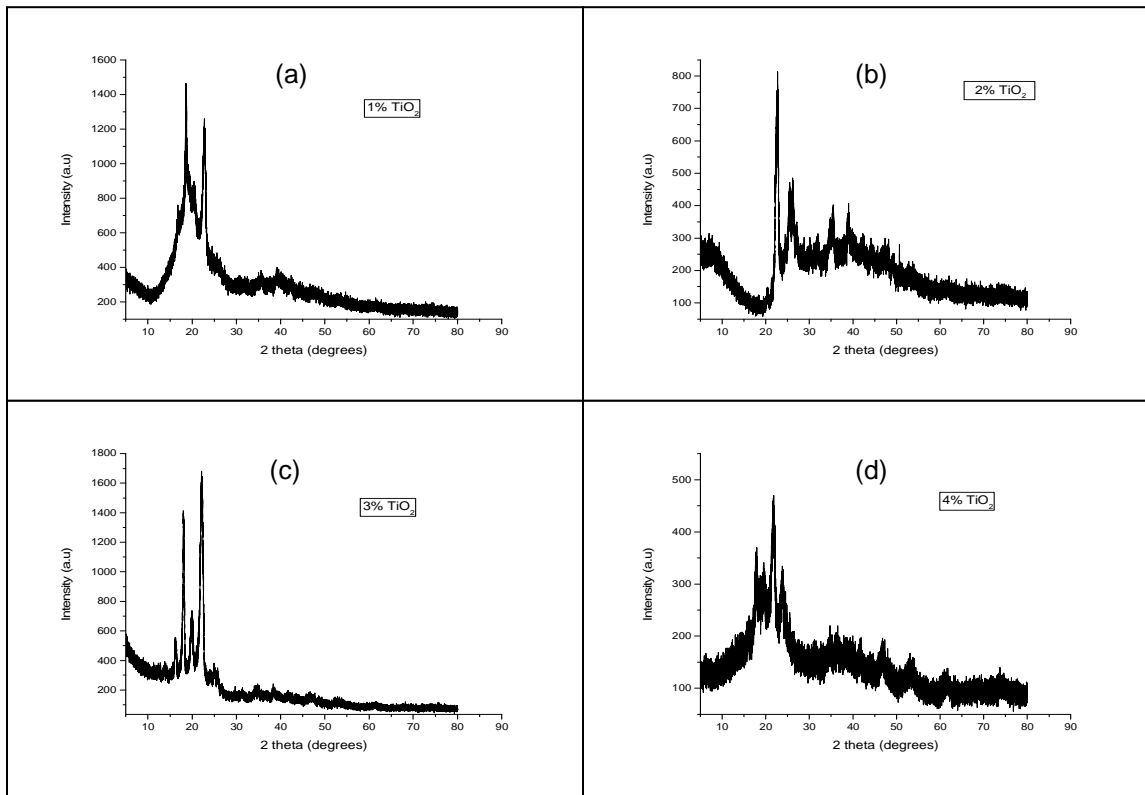
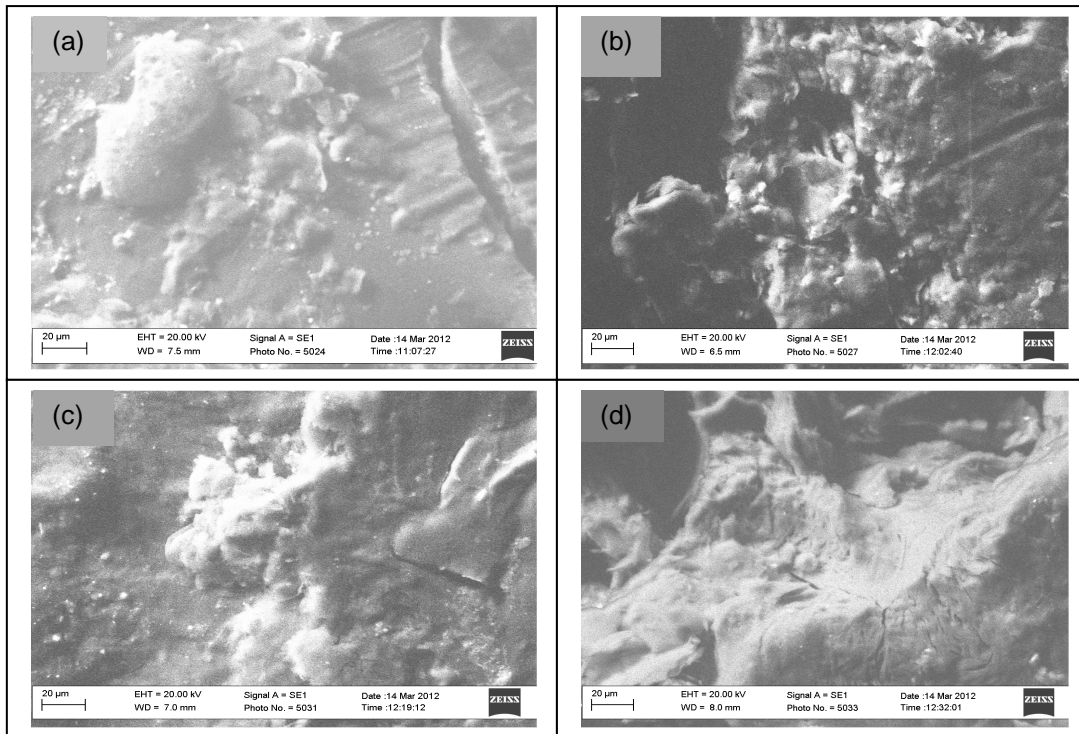


Figure 4: X-ray Diffraction Patterns of Polymer Blend/TiO₂ Nanocomposites containing (a) 1% of TiO₂, (b) 2% of TiO₂, (c) 3% of TiO₂ and (d) 4% of TiO₂.

229 The microstructure of the polymer blend/TiO₂ nanocomposites reveals two distinct phases
230 comprising of lighter modified TiO₂ nanoparticles and dark bulk polymer blend matrix. The
231 lighter modified TiO₂ nanoparticles are evenly dispersed over the dark bulk polymer matrix
232 with spherical shapes and the concentration increased with increasing content of the
233 modified TiO₂ NPs (1%-4%) as depicted in figure 5(a-d). The contrast observed in the SEM
234 images [figure 5(a-d)] arises from atomic number difference, since phases within a material
235 are dependent upon back scattered electron yield and the corresponding atomic number of
236 atoms present within different phases. As such, the modified TiO₂ nanoparticles appear
237 lighter compared to the bulk polymer blend matrix because the atoms present in TiO₂ phase
238 have higher atomic numbers and higher back scattered electron yield. The average particle
239 diameters of the polymer-blend/TiO₂ nanocomposites as determined from SEM images
240 using imaging software (Image J) range from 119±5µm to 179±4µm.

241
242
243
244
245
246
247
248
249
250
251
252



253 Figure 5: SEM Images of Polymer Blend/TiO₂ Nanocomposites containing: (a) 1% of TiO₂,
254 (b) 2% of TiO₂, (c) 3% of TiO₂ and (d) 4% of TiO₂

254

255 It is a well known fact that changes occur when atoms or impurities are incorporated into a
256 pure matrix (polymer, semiconductor, metal etc), because their environment is neither inert
257 nor isotropic. Subsequently, exposing the anisotropic matrix (polymer nanocomposites) to
258 UV-vis light may lead to resonant coupling between the photons (in this case, UV-vis
259 component of the electromagnetic spectrum) and the collective modes (electronic
260 transitions/excitations) of the polymer nanocomposites. The interaction of the UV-visible light
261 with the polymer nanocomposites possibly will give rise to polarization of the nanocomposite
262 matrix, which in turn can be seen as variation in the magnitude of absorption/transmission
263 with respect to changes in wavelengths (i.e. 200-900nm) when examined using UV-vis
264 spectrophotometre. In addition to this, anisotropy of the nanocomposite matrix resulting from
265 addition of TiO₂ nanoparticles gave rise to varied properties as a result of slight structural
266 modifications. These structural modifications have been studied using FTIR, XRD and SEM.

267 The slight variation in the percentage absorbance over wavelength range (i.e. 200-900nm) is
268 attributed to the TiO₂ nanoparticles content (1-4%) in each sample.

269 The UV-VIS spectra of polymer blend/TiO₂ nanocomposites are given in figure 6(a-d) below.
270 The plot for polymer blend/TiO₂ sample (containing 1 wt % of nanoparticles) is presented in
271 figure 6(a). The sample filters at the onset of ultraviolet radiation wavelength through 295nm
272 above which it absorbs significantly and rapidly until maximum absorbance of 1.4% is
273 recorded at a wavelength of 390nm. Slightly above the visible range, there is little decline in
274 absorbance but appreciates reasonably through the whole range with maximum recorded at
275 a wavelength of approximately 500nm. The sample displayed excellent property of being an
276 ultraviolet radiation filter at low wavelengths (<300nm) and absorber at higher wavelengths
277 (300-400nm) of the UV range in addition to being an excellent visible absorber. Figure 6(b)
278 portrays the behaviour for polymer blend sample containing 2 wt % of TiO₂ nanofillers. The
279 spectrum shows absolute transparency from the onset of ultraviolet radiation wavelength
280 range through a visible wavelength of 515nm. A much significant absorbance of
281 approximately 3.0%, the maximum, is recorded slightly above that (i.e. at 520nm) from which
282 the absorbance decreases very slightly with a minimum of 2.7% at 800nm. This material is
283 an excellent UV filter and a very good visible radiation absorber.

284 A similar behaviour to the polymer blend samples described above is observed in both the
285 remaining blend samples (with 3 wt % and 4 wt % of TiO₂ nanofillers respectively) as
286 depicted in figures 6(c) and 6(d). However, there are slight shifts in the onsets of absorption,
287 with the sample containing 3 wt % of TiO₂ having onset at a wavelength of 590nm
288 corresponding to maximum absorbance of approximately 3.0% and that containing 4 wt % of
289 TiO₂ having onset at 550nm corresponding to maximum absorbance of 2.9% as well. The
290 minimum absorbance for these samples are recorded at 795nm (2.8%) and at 780nm (2.7%)
291 respectively. These shifts are attributed to higher content of TiO₂ nanofillers in the polymer
292 blends as TiO₂ as transparent to UV-vis light.
293

294

295

296

297

298

299

300

301

302

303

304

305

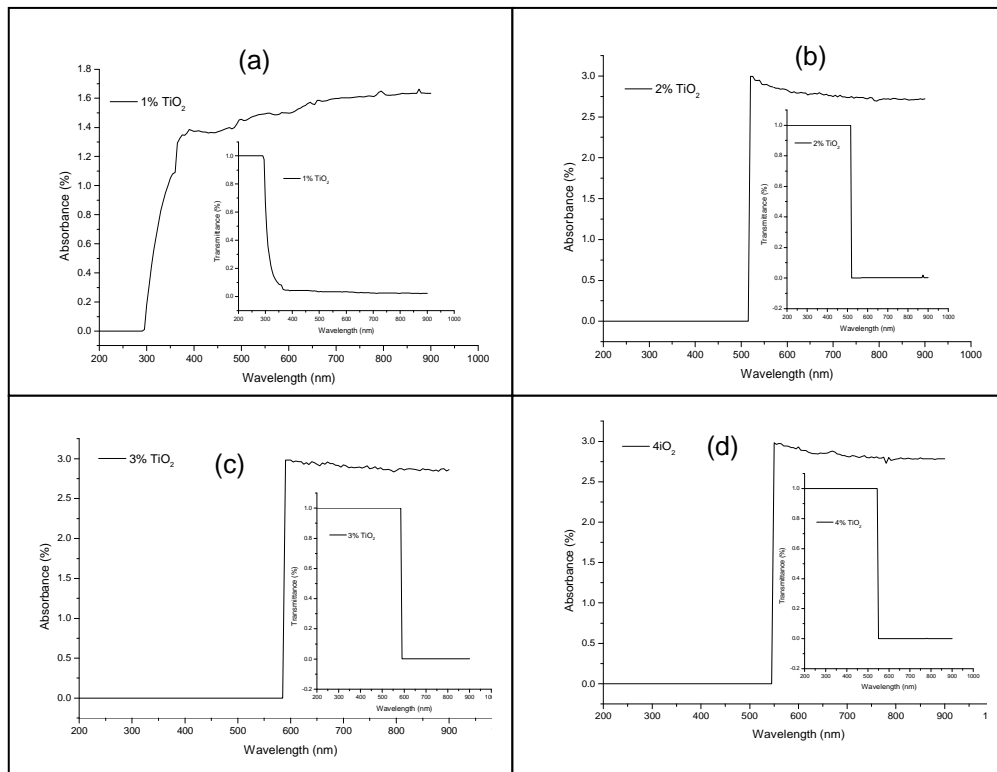


Figure 6: UV-vis spectra of Polymer-Blend/TiO₂ Nanocomposites containing: (a) 1% of TiO₂, (b) 2% of TiO₂, (c) 3% of TiO₂ and (d) 4% of TiO₂.

306 **4. CONCLUSION**

307

308 The development of the polymer blend nanocomposites was realized by surface modification
309 of TiO₂ Nps in order to create functional sites and improve dispersion of nanoparticles in the
310 polymer blend matrices. FTIR spectroscopy proved the existence of covalent chemical
311 bonding between the polymer chains and inorganic phase in the polymer blend
312 nanocomposites. Thus, revealing significant absorptions below 900cm⁻¹ to represent titanium
313 bonds with organic groups and oxygen while other prominent functional groups above
314 900cm⁻¹ reflect the additivity of polyvinyl acetate and polyvinyl alcohol. X-ray diffraction
315 analysis of the polymer blend nanocomposites revealed an increase in the percentage
316 crystallinity from 56.9 ± 0.2% to 67.6 ± 0.7% for the polymer-blend nanocomposites as TiO₂
317 nanoparticles content increases from 1% to 4%. Observations from SEM analysis showed
318 that the dispersion of TiO₂ nanoparticles in the polymer matrix was relatively uniform with
319 particles having good adhesion with polymer domains. Investigation with UV-visible
320 spectrophotometre revealed that the dispersion of TiO₂ nanoparticles improved the optical
321 properties of the polymer blends. The fact that nanocomposites displayed some level of
322 transparency at lower wavelengths indicates that the nanoparticles are not agglomerated. In
323 addition, strong UV absorption in some of the nanocomposite samples was observed
324 because of the incorporated TiO₂ particles. In fact, with the exception of sample with 1%
325 content of nanoparticles, all the samples transmit UV radiation and absorb visible radiation at
326 wavelengths of 520nm, 590nm and 550nm respectively. Thus the developed polymer blend
327 nanocomposites could act as an efficient optically transparent UV filter and visible radiation
328 absorber.

329

330

331 **ACKNOWLEDGEMENTS**

332

333 We thank Physics Advanced Laboratory, Sheda Science and Technology Complex, Abuja,
334 Nigeria, National Research Institute for Chemical Technology, Zaria, Nigeria and the Multi-
335 users Laboratory, Department of Chemistry, Ahmadu Bello University, Zaria, Nigeria for
336 technical assistance during the experimental characterization.

337

338

339

340

341 **COMPETING INTERESTS**

342

343 Authors have declared that no competing interests exist.

344

345

346 **AUTHORS' CONTRIBUTIONS**

347

348 This work was carried out in collaboration between all authors. Authors TOA and POA
349 designed the study. Author TOA wrote the protocol and wrote the first draft while, author
350 TOA and author IA carried out the experimental work and analyses. Author TOA and author
351 IA managed the literature searches. All authors read and approved the final manuscript.

352

353

354 **REFERENCES**

355

356 1. Wanchoo RK, Sharma PK. Viscometric Study on the Compatibility of some Water
357 Soluble Polymer-Polymer Mixtures. *Euro. Polym. J.* 2003; 39: 1481-82.

358 2. Dyson RW. *Engineering Polymers*. Chapman and Hall, New York. 1990: 20-28

359 3. Chuu MS, Meyers RR. Effect of Moisture content on the dielectric behaviour of Poly
360 (vinyl acetate)-Natural Rubber blend. *J Appl Polym Sci.* 1987; 34 (4):1447

361 4. Saujanya C, Radhakrishna S. *Polymer Nanocomposites*, *J. of Polym. Sci.* 2001:
362 42: 6723-6731.

363 5. Riegler J, Ditengou F, Palme K, Nann T. Blue Shift of CdSe/ZnS Nanocrystals-
364 Labels upon DNA-Hybridization. *J. Nanobiotechnol.* 2008; 6(1): 7.

365 6. Bruchez Jr. M, Moronne M, Gin P, Weiss S, Alivisatos AP. Semiconductor
366 Nanocrystals as Fluorescent Biological labels. *Science.* 1998; 281(5385):2013-
367 2016.

368 7. Chan WCW, Nie S. Quantum Dot Bioconjugates for Ultrasensitive Nonisotopic
369 Detection Science. 1998; 281(5385): 2016-2018.

370 8. Jaiswal J, Mattoussi H, Mauro J, Simon S. Long-term multiple Color Imaging of Live
371 Cells Using Quantum Dot Bioconjugates. *Nat. Biotechnol.* 2003; 21(1): 47-51.

372 9. Patra MK, Manoth M, Singh VK, Gowd GS, Choudhry VS, Vadera SR, Kumar N.
373 Synthesis of Stable Dispersion of ZnO Quantum Dots in Aqueous Medium Showing
374 visible Emission from Bluish-Green to Yellow. *J. Lumin.* 2009; 129 (3):320-324.

375 10. Guo Z, Kumar C, Henry LL, Domes EE, Hormes J, Podlaha EJ. Displacement
376 Synthesis of Cu Shells Surrounding Co Nanoparticles. *J. Electrochem. Soc.* 2005:
377 152(1): D1-D5.

378 11. Legrini O, Oliveros E, Braun AM, Photochemical Processes for Water Treatment.
379 *Chem. Rev.* 1993; 93(2): 671-698.

380 12. Sugimoto T, Zhou X, Muramatsu A. Synthesis of Uniform Anatase TiO₂
381 Nanoparticles by Gel-Sol Method: 3. Formation Process & Size Control. *J. Colloid
382 Interface Sci.* 2003; 259(1): 43-52.

383 13. Jiaguo Y, Jimmy CYU, Cheng B, Zhao X. Photocatalytic Activity & Characterization
384 of the Sol-Gel Derived Pb-Doped TiO₂ Thin-films *J. Sol-Gel Sci. Tech.* 2002; 24(1)
385 39-48.

386 14. Bouras P, Stathatos E, Lianos P. Pure versus Metal-ion-doped Nanocrystalline
387 Titania for Photocatalysis. *Appl. Catal. B: Environ.* 2007; 73(1-2): 51-59.

388 15. Lagashetty A, Venkataramen I. *Polymer Nanocomposites*. John Wiley and sons.
389 2005.

- 390 16. Garcia C, Maria M, Dela L. Polymer-Inorganic Nanocomposites: Influence of
391 Colloidal Silica, A PhD thesis submitted to the university of Twente, Netherlands.
392 2004.
- 393 17. Mohan S, Lauren NC, Surya SG, Karen IW. Melt Intercalation of Polystyrene in
394 Layered Silicates, J. of Polym. Sci.: part B: Polym. Physics. 1996: 34: 1433-1449.
- 395 18. Lee SS, Lee CS, Kim MH, Kwak SY, Park M, Lim S, Choe CR, Kim J. Specific
396 Interaction Governing the Melt Intercalation of Clay with Poly(styrene-co-
397 acrylonitrile) Copolymers. J. of Polym. Sci.: part B: Polym. Physics. 2001: 39: 2430-
398 2435.
- 399 19. Pegoretti A, Dorigato A, Penati A. A Tensile Mechanical Response of Polyethylene-
400 Clay Nanocomposites. Express Polymer Letters. 2007: 1(3): 123-131.
- 401 20. Tolstov AL, Matyushov VF, Klymchok, DO. Synthesis and Characterization of Hybrid
402 Cured Poly (ether-urethane) Acrylate/Titania Microcomposites Formed from
403 Tetraalkoxytitanate Precursors, Express Polymer Letters. 2008: 2(6) 449-459.
- 404 21. Manias E, Zhang J, Huh JY. Polyethylene Nanocomposite Heat Sealants with a
405 Versatile Peelable Character, Macromol. Rapid Commun. 2009: 30: 17-23.
- 406 22. Eichhorn S J, Young RJ. The Young's modulus of Microcrystalline cellulose.
407 Cellulose. 2001: 8: 197-207.
- 408 23. Morterra C, Magnacca G. A case Study: Surface Chemistry & Structure of Catalytic
409 Aluminas as Studied by Vibrational Spectroscopy of Adsorbed species" Catal.Today.
410 1996: 27: (3-4): 497-532.
- 411 24. G'eminarada JC, Bonraya DH. Thermal Conductivity Associated with a Bead-Bead
412 Content Decorated by a Liquid Bridge; An Experimental Study Based on the
413 Response of a Chain Subjected to Thermal Cycles. Gayvallet Eur, Phys. 2005:
414 48: 509-517.
- 415 25. Lee GW, Park M, Kim J, Lee JI, Yoon HG. Enhanced thermal conductivity of
416 polymer Composites filled with hybrid filler. Composites Part A: Applied Science and
417 Manufacturing. 2006: 37: 727-734.
- 418 26. Shuqiang J, Hongmin Z. Electrolysis of Ti_2CO Solid Solution Prepared by TiC &
419 TiO_2 , Journal of Alloys & Compounds. 2007: 2007: 438: 243-246.
- 420 27. Yang Z, Choi D, Kerisit S, Rosso KM, Wang D, Zhang Z, Graffi G, Liu
421 J. Nanostructures and Lithium Electrochemical Reactivity of Lithium titanates and
422 Titanium oxides: A Review. Journal of Power Sources. 2009: 192(2): 588-598.
- 423 28. Patterson AL. The Scherrer formula for X-ray particle size determination. Physical
424 Review. 1939: 56(10): 978-982.
- 425
426
427
428
429